Published in final edited form as:

Biol Psychiatry. 2019 June 15; 85(12): 1001–1010. doi:10.1016/j.biopsych.2019.02.007.

The selective RhoA inhibitor Rhosin promotes stress resiliency through enhancing D1-MSN plasticity and reducing hyperexcitability

T. Chase Francis[1,2], **Alison Gaynor**[1], **Ramesh Chandra**[1], **Megan E. Fox**[1], **Mary Kay Lobo**[1,*]

[1]Department of Anatomy and Neurobiology, University of Maryland School of Medicine, Baltimore, MD, USA

[2]Synaptic Plasticity Section, National Institute on Drug Abuse Intramural Research Program, Baltimore, MD, USA

Abstract

Background: Nucleus Accumbens (NAc) dopamine 1 receptor medium spiny neurons (D1-MSNs) play a critical role in the development of depression-like behavior in mice. Social defeat stress causes dendritic morphological changes on this MSN subtype through expression and activation of early growth response 3 (EGR3) and the Rho GTPase RhoA. However, it is unknown how RhoA inhibition affects electrophysiological properties underlying stress-induced susceptibility.

Methods: A novel RhoA specific inhibitor, Rhosin, was utilized to inhibit RhoA activity following chronic social defeat stress. Whole-cell electrophysiological recordings of D1-MSNs were performed to assess synaptic and intrinsic consequences of Rhosin treatment on stressed mice. Additionally, recorded cells were filled and analyzed for their morphological properties.

Results: We found RhoA inhibition prevents both D1-MSN hyperexcitability and reduced excitatory input to D1-MSNs caused by social defeat stress. NAc specific RhoA inhibition is capable of blocking susceptibility caused by D1-MSN EGR3 expression. Lastly, we found Rhosin enhances spine density, which correlates with D1-MSN excitability, without affecting overall dendritic branching.

Conclusions: These findings demonstrate pharmacological inhibition of RhoA during stress drives an enhancement of total spine number in a subset of NAc neurons that prevents stress-related electrophysiological deficits and promotes stress resiliency.

[*]Correspondence to: Mary Kay Lobo, Ph.D., University of Maryland School of Medicine, Department of Anatomy and Neurobiology, 20 Penn Street, HSF2, Rm 265, Baltimore, MD 21201, mklobo@som.umaryland.edu.

Disclosures

The authors report no biomedical financial interests or potential conflicts of interest.

Keywords

Stress resilience; Social defeat stress; Nucleus Accumbens; Medium Spiny Neuron; RhoA; Intrinsic excitability

Introduction

Depression is prevalent globally and pharmacological treatments for depressed patients vary in their efficacy. Devising new treatments to specifically target functional changes in core brain loci that drive depression, such as the nucleus accumbens (NAc) (1–3), would provide enhanced treatment outcomes. The NAc contains a diverse set of neurons, the majority of which are NAc efferents termed medium spiny neurons (MSNs). These cells are differentiated by their dopamine receptor expression, either D1 receptor or D2 receptor expression and their activity plays differential roles in reward related behaviors (4–8). D1-MSNs are critical for the expression of anhedonia, a core behavioral symptom in depression (5, 9–11). In response to repeated stress, these neurons display electrophysiological adaptations including hyperexcitability, reduced excitatory transmission, and reduced activity (10, 12, 13). D1-MSN electrophysiolgical changes appear to be driven by alterations in dendritic morphology (10). Indeed, in rodents (14) and depressed patients (15), the NAc displays significant reductions in volume. It is possible these volumetric changes could be driven by D1-MSN dendritic atrophy (10, 11).

Depression-like behavior caused by chronic stress can be alleviated by blocking both electrophysiological and morphological changes via knockdown of early growth response 3 (EGR3) which regulates neuronal plasticity (4, 16–20). EGR3 binds and targets molecules which drive structural complexity in MSNs, including the Rho-GTPase RhoA (10). RhoA has been shown to be critically involved in mediating behavioral deficits to social defeat stress (11). However, it is unknown what the effects of RhoA inhibition are on electrophysiological properties underlying depression-like behavior and the relationship between these changes on structural properties in D1-MSNs.

Here, we utilized a novel, small molecule Rho-GTPase inhibitor Rhosin, which selectively targets RhoA (21). By inhibiting RhoA, Rhosin prevents negative cytoskeletal reorganization (22–24) and formation of protrusions such as filopodia without toxic effects (25). We replicate the finding that systemic and NAc specific RhoA inhibition blunts behavioral deficits caused by social defeat stress (11). We demonstrate this stress-resilience relies on restoration of NAc D1-MSN electrophysiological properties underlying depression-like behavior. Additionally, we establish a role for enhanced dendritic spine formation caused by RhoA inhibition in blunting D1-MSN hyperexcitability and preventing depression-like behavior.

Materials and Methods

Experimental Subjects

For all electrophysiology and morphological experiments, D1-GFP or D2-GFP hemizygote mice on a C57BL/6J background were utilized (26) (gensat.org). Drd1a-Cre (D1-Cre)

hemizygote mice (line FK150) (27) were used in EGR3 overexpression experiments. For behavioral experiments including sucrose preference, C57Bl6/J (Jackson) mice were used. All experimental mice were male at 8–12 weeks of age. Male CD-1 retired breeders (Charles River, >4 months), screened for high aggression, were used as aggressors. Studies were conducted in accordance with IACUC at UMSOM guidelines.

Social Defeat Stress and Sucrose Preference

Chronic social defeat stress (CSDS) was performed as previously described (10, 12, 28). Briefly, each day for 10 days, mice were placed in a cage containing a novel aggressive CD-1 retired breeder for 10 min of physical interaction followed by 24 hrs of sensory interaction until the next defeat session. Subthreshold social defeat stress (SSDS) was performed as previously described (10, 12). Over the course of 1 day, mice were exposed to three novel CD-1 aggressors for 2 min per defeat session with 15 min of sensory contact after each defeat session. Social interaction behavior was quantified on day 11 (CSDS) or the day after SSDS and tracked for offline analysis (CleverSys, Reston, VA, USA). Social interaction behavior was performed by placing mice in an open field with an empty perforated box which they were allowed to explore for 2.5 min. Immediately after, defeat mice were removed and a novel CD-1 retired breeder was added to the perforated chamber and defeat mice were again placed in the open field (2.5 min) and time mice spent in an interaction zone around a perforated box was quantified.

Two-bottle choice sucrose preference was administered as it was previously (10). Mice were habituated for 2 days to two 50 mL bottles filled with water. On the third day, one water bottle was replaced with a 1% sucrose solution. Bottles were weighed and switched to the opposite side daily. Preference was calculated as percentage of sucrose consumed relative to total liquid consumed over the two day sucrose consumption period.

Animal Surgery and Rhosin Administration

For EGR3 overexpression (OE) experiments, adeno-associated virus (AAV) injection was performed as described previously (10) under 0.5–1.5% isoflurane anesthesia. For reference to AAV construction see Chandra et al. (29). The cre-dependent, double inverted open reading frame (DIO) virus (AAV-DIO-EGR3-eYFP) was injected bilaterally (0.6 μL at a rate of 50 nL/minute) in the NAc (A/P: 1.6 mm, Lat: 1.5 mm, D/V:−4.4 mm) of D1-Cre mice. For Rhosin NAc infusion experiments, 4.0mm bilateral cannulas (Plastics One, Roanoke, VA) were placed above the NAc and affixed with bone screws and dental cement. Notes of cannula placement were taken when mice were sacrificed the day after social interaction. Only mice with cannula tracts above or within the NAc were included in the analysis. Mice recovered in their home cage on heating pads until fully ambulatory. All mice were monitored daily and allowed two weeks to recover in the animal facility before behavioral testing.

Rhosin was prepared in a 5% DMSO, 0.9% saline solution, gently warmed to dissolve. Vehicle contained a 5% DMSO solution in 0.9% saline. Injections were administered intraperotoneally (i.p.) at 40 mg/kg 15 min prior to physical defeat. For Rhosin administered following defeat, injections were administered one time per day for 7 days and social

interaction was retested on day 8. For cannula infusion, 30 μM Rhosin solution was infused bilaterally at a rate of 0.1 μL per minute for a total 0.5 μL infusion on each side.

Immunohistochemistry

Mice expressing EGR3-eYFP were perfused with 4% paraformaldehyde (PFA) and incubated in PFA overnight and placed in 30% sucrose solution for cryoprotection. Brain slices (35μm) were sectioned by cryostat (Leica). Slices were washed 3 times for 10 min with 1X phosphate buffered solution (PBS). Slices were blocked in 3% normal donkey serum and 0.3% Triton-X (20%) in 1X PBS. Slices were incubated in rabbit GFP (1:1000; Aves Lab) primary antibody overnight at room temperature. The next day, slices were washed 3 times for 15 min and incubated in anti-rabbit Alexa 488 (1:1000; Jackson Immuno) for 2 hrs followed by 1X PBS and mounting with Vectashield DAPI-containing mounting media. All slices were imaged on a FV500 confocal microscope (Olympus).

Slice Processing and Dendrite Analysis

Slices and cells were processed and analyzed as previously described (10). Briefly, cells were filled with neurobiotin (0.1%) during whole cell recording and slices were immediately fixed in 4% PFA following recording. Slices were washed with 1X phosphate buffered solution (PBS) and blocked in in 10% normal donkey serum and 0.05% Triton X (20%). Slices were incubated overnight in Steptavidin conjugated to Cy3 (Jackson Immuno; #016-160-084). Slices were washed in 1X PBS and mounted the next day. For dendritic arbor analysis, Z-stacks were reconstructed with the ImageJ plugin (NIH, Bethesda, MD) simple neurite tracer (30). Sholl analysis was performed by counting dendrite intersections with concentric circles. For spines, spines were classified and analyzed using NeuronStudio (MSSM, CNIC). Spine counts from secondary dendrites (2–3 per cell) were averaged per cell. 1–2 cells per animal were used for dendrite analysis. For all counts, the experimenter was blind to behavioral conditions.

Electrophysiology

Isoflurane-anesthetized mice were perfused with, and NAc coronal slices (300 μm) were prepared in ice cold oxygenated sucrose artificial cerebrospinal fluid (ACSF) containing (mM: 194 sucrose, 30 NaCl, 26 $NaHCO_3$, 10 Glucose, 4.5 KCl, 3 $MgCl_2$, 1.2 NaH_2PO_4, osmolarity 330mOsm). Slices were incubated at 33°C for 1hr before recording in holding ACSF (mM: 125 NaCl, 25 $NaHCO_3$, 10 Glucose, 3.5 KCl, 3 $MgCl_2$, 1.25 NaH_2PO_4, 0.1 $CaCl_2$, osmolarity 305–310mOsm). Sucrose cutting solutions provide a protective cutting method for protection of neurons and provide improved health of striatal neurons relative to sodium-based ACSF solutions (31). For recording, magnesium and calcium in ACSF were 1 mM. Whole-cell recordings were performed under DIC visual guidance at 40x using an Olympus BX61 microscope (Olympus, Center Valley, PA, USA). D1-MSNs or D2-MSNs were identified by visualizing GFP positive or GFP negative cells using a mercury arc lamp and a GFP filter. Negative cells were verified to be MSNs by action potential waveforms, low resting membrane potential, and lack of spontaneous firing at baseline. Signals were amplified and digitized using a Mulitclamp 700B amplifier and Digidata 1322 digitizer (20 kHz), respectively (Molecular Devices, Sunnyvale, CA USA).

Whole-cell recordings utilized a potassium gluconate based internal solution (mM: 126 K Gluconate, 10 HEPES, 4 KCl, 2 ATP-Mg, 2 Na2ATP, 0.3 GTP, 0.2 EGTA, osmolarity 285 mOsm) to fill borosilicate glass pipettes (2–4 MΩ). Rheobase was obtained by injecting a 1 sec pulse-ramp. Capacitance was determined by examining charge in capacitive transients in voltage clamp (holding −70 mV) with a +5 mV, 500 ms voltage deflection (32). Spontaneous excitatory post synaptic potentials (sEPSPs) were acquired following 5min of cell stabilization prior to excitability recordings. Spontaneous events were deemed to be excitatory by bath application of the α-amino-3-hydroxy-5-methyl-4-isoxazolepropionic acid (AMPA) receptor antagonist 6-cyano-7-nitroquinoxaline-2,3-dione (CNQX, 10 μM) and the N-methyl-D-aspartate (NMDA) receptor antagonist APV (50 μM).

RhoA Activation Assay

RhoA activation was determined using a G-LISA (Cytoskeleton, #BK124, Denver, CO, USA) as previously described (11). Briefly, tissue was acquired 2 hrs following a 40 mg/kg injection of Rhosin followed by a single defeat. NAc tissue punches using 14-G needles were homogenized with a Pellet Pestle (Thermo Fisher) in lysis buffer, homogenates were centrifuged, and supernatants were snap frozen at −80°C. Protein concentrations were equalized with lysis buffer and active RhoA determined according to manufacturer's instructions.

Statistical Analysis

Statistics were tabulated using Graphpad Prism 5.0 software. For all four group experiments, two-way ANOVAs were used followed by Bonferroni post-hoc tests corrected for multiple comparisons. A repeated-measures two-way ANOVA was used for the spike vs. current injection plot. *P*-value in the legend statistics report interaction results unless otherwise specified. Significance on graphs were derived from post-hoc tests (*$p<0.05$, **$p<0.01$, ***$p<0.001$, ****$p<0.0001$). For two group statistics, two-tailed *t*-tests were used. For cumulative probability plots, Kolmogorov–Smirnov tests were used between groups to calculate differences between distributions. In graphs, individual points represent number of: mice in all behavioral experiments; cells in electrophysiological experiments (N/n=Mice/cells); and cells in morphology experiments. All graphs are represented as mean ± standard error measure. Exact statistics can be found in Supplemental Table 1.

Results

Previously, we observed RhoA is critically involved in mediating behavioral outcomes to social defeat stress (11). To first determine if the RhoA inhibitor Rhosin would traffic to and be functional in the brain, we injected mice with vehicle or Rhosin (40 mg/kg, i.p.) 15min prior to a single 10 min defeat session and collected NAc tissue punches 2 hrs following the defeat. Active RhoA was significantly reduced in mice injected with Rhosin compared to vehicle controls (Supplemental Figure 1A). Next, we characterized general ambulatory and anxiety-like behaviors in response to Rhosin injection by analyzing behavior in an open field. No behavioral differences were observed following Rhosin compared to vehicle injected mice (Supplemental Figure 1B–E).

A 10 day CSDS procedure was performed on mice destined for electrophysiology or follow up behavioral measures (Figure 1A). Rhosin (40 mg/kg, i.p.) or vehicle was systemically administered 15 min prior to defeat to block RhoA activation. While defeat significantly reduced the time that experimental mice spent interacting with a novel mouse, Rhosin administration suppressed this effect (Figure 1B) without affecting locomotor behaviors (Figure 1C). A lower dose of Rhosin (20 mg/kg, i.p.) was not capable of blocking defeat-induced susceptibility (Supplementary Figure 2A). Additionally, Rhosin blocked sucrose preference deficits induced by defeat (Figure 1D). Rhosin alone in the absence of defeat did not affect interaction behavior or sucrose preference (Figure 1B,D). Rhosin (40 mg/kg, i.p.) administered one time per day for 7 days following social interaction did not reverse deficits due to social defeat stress (Supplementary Figure 2B), suggesting Rhosin blocks the alterations due to social defeat, but likely does not reverse alterations already caused by CSDS.

Next, to determine if NAc RhoA inhibition could promote resilience to CSDS, the NAc of mice were cannulated and mice were exposed to CSDS (Figure 2A). 15 min prior to defeat, mice received bilateral, intra-NAc infusions of Rhosin (30 μM) and then were subjected to physical defeat. Rhosin infusion was sufficient to attenuate avoidance behavior (Figure 2B). Previously, we found overexpression of EGR3 in NAc D1-MSNs was sufficient to promote susceptibility to social defeat stress (10). Two weeks following viral injection and overexpression of EGR3 in D1-MSNs, mice were subjected to SSDS, a defeat paradigm that normally does not induce depression-like behavior except in vulnerable populations (Figure 2C) (10, 12, 28). Vehicle or Rhosin (40 mg/kg, i.p.) was injected 15 min prior to the first physical defeat. Rhosin injection was capable of blocking susceptibility caused by EGR3 overexpression (OE) in D1-MSNs, suggesting RhoA inhibition is capable of suppressing NAc EGR3-induced susceptibility.

CSDS causes a persistent (i.e., at least 1 month) enhancement in D1-MSN excitability which corresponds to depression-related behavioral changes (10, 12, 33). To determine if systemic Rhosin was capable of preventing this effect, we prepared coronal NAc slices from mice that underwent CSDS and received vehicle or Rhosin injections (Figure 1) and recorded from D1-MSNs. Enhanced excitability caused by CSDS was blocked by Rhosin administration as observed by spiking due to current injection (Figure 3A) and rheobase (Figure 3B). As we found previously, rheobase significantly correlated with time in the interaction zone (Figure 3C) (4). Additionally, the increase in input resistance induced by CSDS was blocked by Rhosin administration (Figure 3D). Smaller plateau currents by negative current injection were observed in defeat vehicle treated but not Rhosin treated mice (Figure 3E). This result suggests enhanced input resistance and excitability could be due to a putative potassium channel effect as discussed previously (10). Surprisingly, capacitance still remained reduced in both CSDS vehicle and Rhosin treated mice (Figure 3F), indicating dendritic structural changes may not dictate intrinsic electrophysiological measures. In line with this finding, Rhosin was not capable of restoring dendritic complexity in defeated mice (Figure 4A–B). Additionally, total dendritic length (Figure 4C) and dendritic branch points remained unchanged by Rhosin administration (Figure 4D). No change in soma diameter was found (Figure 4E). These results suggest changes in rheobase caused by defeat might mediated by an alternative mechanism that is not dependent on dendritic complexity.

Previously, we found spontaneous excitatory input was reduced by CSDS in D1-MSNs (10, 12). To assess the impact of systemically administered Rhosin on excitatory input, we analyzed spontaneous excitatory post-synaptic potentials (sEPSPs) prior to acquisition of excitability data. Spontaneous input was deemed to be excitatory as bath application of the AMPA receptor blocker CNQX and the NMDA receptor blocker APV was sufficient to block all spontaneous input (Figure 5A). As observed previously, the frequency of spontaneous excitatory input on NAc D1-MSNs was significantly reduced by CSDS (Figure 5B–C), but did not directly correlate with behavior (Supplemental Figure 3) (4). However, Rhosin administration blocked this effect completely. Defeat significantly enhanced amplitude of sEPSPs, but was blocked by Rhosin injection (Figure 5D). Since recordings took place in a potassium based internal solution, input resistance was increased (Figure 3D), and potassium channel currents were decreased by CSDS (Figure 3E), the enhancement in sEPSP amplitude was likely governed by enhanced input resistance. Additionally, this interpretation is consistent with previous reports of no change in D1-MSN mEPSC amplitude (Francis et al 2015, 2017).

Control of excitatory input is, in part, driven by spine density. To determine if restoration in excitatory transmission and excitability was due to changes in spines, we classified spine types by morphology and quantified the density of spines in all groups. Systemic Rhosin administration significantly enhanced overall spine density in defeated mice as compared to vehicle treated mice (Figure 6A–B). This enhancement was driven by an increase in thin and mushroom spine density (Figure 6C). Interestingly, rheobase significantly correlated with total spine density (Figure 6D), suggesting enhanced spine density may play a role in suppressing hyperexcitability caused by CSDS.

Discussion

We have found that selective RhoA inhibition via a novel RhoA inhibitor, Rhosin, can prevent susceptibility to social defeat stress by suppressing stress-induced NAc D1-MSN enhanced excitability and reduced excitatory input. Rhosin prevents electrophysiological changes by enhancing overall spine number, as observed by enhanced spine density. Additionally, this work has demonstrated NAc EGR3 and RhoA may interact to facilitate susceptibility and RhoA inhibition can prevent enhanced susceptibility caused by enhanced EGR3 expression. This is consistent with our previous study demonstrating an enrichment of EGR3 binding on the RhoA promoter suggesting direct transcriptional regulation of RhoA after social defeat stress (10). Additional studies will be necessary to determine whether the direct enhancement of RhoA expression or expression of other facilitatory RhoA signaling molecules drives enhanced RhoA activity through this EGR3 mechanism.

Previous work demonstrated a RhoA-dependent reduction in NAc dendritic complexity accounts for behavioral effects of social defeat stress (11). While the current findings do not show an overall restoration in dendritic arbor, enhanced spine density is observed. It is likely that the total number of spines, whether through enhanced density of spines or enhanced overall spines by increasing dendritic branching is sufficient to bring about the same behavioral effect. For instance, alterations in dendritic arbor on prefrontal cortical neurons caused by stress greatly reduce overall excitatory input, weakening cortical networks (34–

36). Driving NAc excitatory afferents or altering excitatory plasticity can reverse physiological and behavioral outcomes to different stress paradigms in a D1-MSN-specific manner (4, 37). Therefore, by enhancing overall excitatory activity optogenetically (38) or by transcranial magnetic stimulation (39), both which produce anti-depressant effects, it may be possible to compensate for reduced excitation thereby normalizing behavior. Analogously, enhancing activity of D1-MSNs optogenetically can promote anti-depressant effects (12). Therefore, it is possible the enhancement in NAc spine density by RhoA may be facilitating similar levels of excitation and it would be interesting to determine if RhoA inhibition specifically suppresses D1-MSN synaptic plasticity caused by stress at specific excitatory synapses within the NAc. Additionally, we found, along with the immature thin spine density enhancement, mushroom spine density was significantly increased. Mushroom spines observed following induction of long-term potentiation (40), are more stable, and underlie learning (41, 42). In the striatum, increasing the number of stable mushroom spines may provide a means of stabilizing salient, emotional memories (40). Since RhoA plays an antagonistic role in spine formation (43), perhaps a larger proportion of spines are allowed to grow and stabilize over the course of Rhosin injections providing stronger excitation to D1-MSNs. This has been previously observed in resilient mice which display stronger synaptic strength on mushroom spines in D1-MSNs (44).

MSN subtypes respond and adapt differentially to stress (4, 5, 9, 37). Often, diametric molecular mechanisms drive physiological and behavioral differences in these subtypes (4). For instance, expression of deltaFosB can oppositely alter plasticity in MSN subtypes and enhance spine density in D1-MSN subtypes (45), which may contribute to the reversal of depressive-like behavior (46) or resilience to stress (47) in a similar manner as we observed. Previous studies have shown a total increase in spine density in mice susceptible to CSDS (48). Our study focuses specifically on spines in D1-MSNs, which may differ from spine density measures on D2-MSNs. We predict the total enhancement in spine density observed in the NAc may be due to enhanced spine density on D2-MSNs, which is consistent with an increase in miniature excitatory post-synaptic current frequency (5). In D1-MSNs, overall alterations in dendritic structure may play a larger role in mediating physiological and behavioral outcomes to stress.

A critical feature in driving anhedonia is reduced excitatory transmission to NAc D1-MSNs (9, 10, 12) and D1-MSN activity drives reward (6, 7). *In vivo* D1-MSN activity is diminished following social defeat stress (10) and this attenuation in activity may be driven by an overall reduction in the frequency of excitatory input caused by a loss in the total number of spines. However, reduced excitatory transmission does not directly correlate with stress-induced avoidance (4). Excitatory input and intrinsic excitability coordinate to produce behavior and output from neurons (49). It is possible that a homeostatic mechanism of restoring normal excitatory input in Rhosin treated mice was sufficient to block hyperexcitability of NAc D1-MSNs. Indeed, rheobase significantly correlates with spine density suggesting enhanced excitatory input onto dendritic spines may prevent hyperexcitability caused by stress. Nevertheless, it is unknown whether changes in excitatory plasticity drive intrinsic changes or vice versa. Future studies will need to examine causal mechanisms linking these two plasticity mechanisms, and their effects on MSN output to connected brain regions. Overall, this study demonstrates an alternative means of restoring

electrophysiological properties of D1-MSNs through enhancing overall spine number and excitatory input through inhibition of RhoA.

Rhosin-mediated RhoA inhibition provides a novel means of suppressing behavioral and physiological changes caused by stress without causing deleterious effects in non-stressed mice. While we did not observe a reversal of depression-like behavior in animals treated with Rhosin following stress, Rhosin treatment during stressful events is effective in driving resilience through a physiologically distinct manner. That is, administration prior to stressful events caused an increase in spine density relative to non-stressed conditions which normalized excitability. Therefore, Rhosin treatment and RhoA inhibition may promote behavioral resilience by allowing for positive actin mobilization and spine formation during stressful events. Rhosin may provide a novel treatment to promote resilience to stress.

Supplementary Material

Refer to Web version on PubMed Central for supplementary material.

Acknowledgements

This work was supported by NIMH R01MH106500 (MKL), NIDA R01DA038613 (MKL), The One Mind/ Janssen Rising Star Translational Research Award (MKL), NIMH F32MH116574 (MEF), and a NIGMS PRAT award 1FI2GM128622–01 (TCF).

References

1. Nestler EJ, Barrot M, DiLeone RJ, Eisch AJ, Gold SJ, Monteggia LM (2002): Neurobiology of depression. Neuron 34: 13–25. [PubMed: 11931738]
2. Floresco SB (2015): The nucleus accumbens: an interface between cognition, emotion, and action. Annu Rev Psychol 66: 25–52. [PubMed: 25251489]
3. Russo SJ, Nestler EJ (2013): The brain reward circuitry in mood disorders. Nat Rev 14: 609–625.
4. Francis TC, Lobo MK (2017): Emerging Role for Nucleus Accumbens Medium Spiny Neuron Subtypes in Depression. Biol Psychiatry 81: 645–653. [PubMed: 27871668]
5. Francis TC, Chandra R, Friend DM, Finkel E, Dayrit G, Miranda J, et al. (2015): Nucleus accumbens medium spiny neuron subtypes mediate depression-related outcomes to social defeat stress. Biol Psychiatry 77: 212–222. [PubMed: 25173629]
6. Calipari ES, Bagot RC, Purushothaman I, Davidson TJ, Yorgason JT, Pena CJ, et al. (2016): In vivo imaging identifies temporal signature of D1 and D2 medium spiny neurons in cocaine reward. Proc Natl Acad Sci U S A 113: 2726–2731. [PubMed: 26831103]
7. Lobo MK, Covington HE 3rd, Chaudhury D, Friedman AK, Sun H, Damez-Werno D, et al. (2010): Cell type-specific loss of BDNF signaling mimics optogenetic control of cocaine reward. Science 330: 385–390. [PubMed: 20947769]
8. Lobo MK, Nestler EJ (2011): The striatal balancing act in drug addiction: distinct roles of direct and indirect pathway medium spiny neurons. Front Neuroanat 5: 41. [PubMed: 21811439]
9. Lim BK, Huang KW, Grueter BA, Rothwell PE, Malenka RC (2012): Anhedonia requires MC4R-mediated synaptic adaptations in nucleus accumbens. Nature 487: 183–189. [PubMed: 22785313]
10. Francis TC, Chandra R, Gaynor A, Konkalmatt P, Metzbower SR, Evans B, et al. (2017): Molecular basis of dendritic atrophy and activity in stress susceptibility. Mol Psychiatry 1–8. [PubMed: 27994236]
11. Fox ME, Chandra R, Menken MS, Larkin EJ, Nam H, Engeln M, et al. (2018): Dendritic remodeling of D1 neurons by RhoA/Rho-kinase mediates depression-like behavior. Mol Psychiatry . 10.1038/s41380-018-0211-5.

12. Francis TC, Chandra R, Friend DM, Finkel E, Dayrit G, Miranda J, et al. (2015): Nucleus accumbens medium spiny neuron subtypes mediate depression-related outcomes to social defeat stress. Biol Psychiatry 77: 212–222. [PubMed: 25173629]
13. Christoffel DJ, Golden SA, Dumitriu D, Robison AJ, Janssen WG, Ahn HF, et al. (2011): IkappaB kinase regulates social defeat stress-induced synaptic and behavioral plasticity. J Neurosci 31: 314–321. [PubMed: 21209217]
14. Anacker C, Scholz J, O'Donnell KJ, Allemang-Grand R, Diorio J, Bagot RC, et al. (2016): Neuroanatomic Differences Associated with Stress Susceptibility and Resilience. Biol Psychiatry 79: 840–849. [PubMed: 26422005]
15. Drevets WC, Videen TO, Price JL, Preskorn SH, Carmichael ST, Raichle ME (1992): A functional anatomical study of unipolar depression. J Neurosci 12: 3628–3641. [PubMed: 1527602]
16. Kim JH, Roberts DS, Hu Y, Lau GC, Brooks-Kayal AR, Farb DH, Russek SJ (2012): Brain-derived neurotrophic factor uses CREB and Egr3 to regulate NMDA receptor levels in cortical neurons. J Neurochem 120: 210–219. [PubMed: 22035109]
17. Roberts DS, Hu Y, Lund I V, Brooks-Kayal AR, Russek SJ (2006): Brain-derived neurotrophic factor (BDNF)-induced synthesis of early growth response factor 3 (Egr3) controls the levels of type A GABA receptor alpha 4 subunits in hippocampal neurons. J Biol Chem 281: 29431–29435. [PubMed: 16901909]
18. Li L, Carter J, Gao X, Whitehead J, Tourtellotte WG (2005): The neuroplasticity-associated arc gene is a direct transcriptional target of early growth response (Egr) transcription factors. Mol Cell Biol 25: 10286–10300. [PubMed: 16287845]
19. Li L, Yun SH, Keblesh J, Trommer BL, Xiong H, Radulovic J, Tourtellotte WG (2007): Egr3, a synaptic activity regulated transcription factor that is essential for learning and memory. Mol Cell Neurosci 35: 76–88. [PubMed: 17350282]
20. Gallitano-Mendel A, Izumi Y, Tokuda K, Zorumski CF, Howell MP, Muglia LJ, et al. (2007): The immediate early gene early growth response gene 3 mediates adaptation to stress and novelty. Neuroscience 148: 633–643. [PubMed: 17692471]
21. Shang X, Marchioni F, Sipes N, Evelyn CR, Jerabek-Willemsen M, Duhr S, et al. (2012): Rational design of small molecule inhibitors targeting RhoA subfamily Rho GTPases. Chem Biol 19: 699–710. [PubMed: 22726684]
22. Zhang XE, Adderley SP, Breslin JW (2016): Activation of rhoa, but not rac1, mediates early stages of s1p-induced endothelial barrier enhancement. PLoS One 11: 1–18.
23. Duan X, Zhang Y, Chen KL, Zhang HL, Wu LL, Liu HL, et al. (2018): The small GTPase RhoA regulates the LIMK1/2-cofilin pathway to modulate cytoskeletal dynamics in oocyte meiosis. J Cell Physiol 233: 6088–6097. [PubMed: 29319181]
24. Zaritsky A, Tseng Y-Y, Rabadán MA, Krishna S, Overholtzer M, Danuser G, Hall A (2017): Diverse roles of guanine nucleotide exchange factors in regulating collective cell migration. J Cell Biol 216: 1543–1556. [PubMed: 28512143]
25. Stakaitytė G, Nwogu N, Dobson SJ, Knight LM, Wasson CW, Salguero FJ, et al. (2018): Merkel Cell Polyomavirus Small T Antigen Drives Cell Motility via Rho-GTPase-Induced Filopodium Formation. (Banks L., editor) J Virol 92 Retrieved from http://jvi.asm.org/content/92/2/e00940-17.abstract.
26. Gong S, Zheng C, Doughty ML, Losos K, Didkovsky N, Schambra UB, et al. (2003): A gene expression atlas of the central nervous system based on bacterial artificial chromosomes. Nature 425: 917–925. [PubMed: 14586460]
27. Gong S, Doughty M, Harbaugh CR, Cummins A, Hatten ME, Heintz N, Gerfen CR (2007): Targeting Cre recombinase to specific neuron populations with bacterial artificial chromosome constructs. J Neurosci 27: 9817–9823. [PubMed: 17855595]
28. Berton O, Mcclung CA, Dileone RJ, Krishnan V, Renthal W, et al. (2006): Essential Role of BDNF in the Mesolimbic Dopamine Pathwayin Social Defeat Stress. Science 864: 1–5.
29. Chandra R, Francis TC, Konkalmatt P, Amgalan A, Gancarz AM, Dietz DM, Lobo MK (2015): Opposing role for Egr3 in nucleus accumbens cell subtypes in cocaine action. J Neurosci 35: 7927–7937. [PubMed: 25995477]

30. Longair MH, Baker DA, Armstrong JD (2011): Simple Neurite Tracer: open source software for reconstruction, visualization and analysis of neuronal processes. Bioinformatics 27: 2453–2454. [PubMed: 21727141]

31. Ting JT, Daigle TL, Chen Q, Feng G (2014): Acute brain slice methods for adult and aging animals: application of targeted patch clamp analysis and optogenetics. Methods Mol Biol 1183: 221–242. [PubMed: 25023312]

32. Golowasch J, Thomas G, Taylor AL, Patel A, Pineda A, Khalil C, Nadim F (2009): Membrane Capacitance Measurements Revisited: Dependence of Capacitance Value on Measurement Method in Nonisopotential Neurons. J Neurophysiol 102: 2161–2175. [PubMed: 19571202]

33. Krishnan V, Han MH, Graham DL, Berton O, Renthal W, Russo SJ, et al. (2007): Molecular adaptations underlying susceptibility and resistance to social defeat in brain reward regions. Cell 131: 391–404. [PubMed: 17956738]

34. Radley JJ, Rocher AB, Miller M, Janssen WG, Liston C, Hof PR, et al. (2006): Repeated stress induces dendritic spine loss in the rat medial prefrontal cortex. Cereb cortex 16: 313–320. [PubMed: 15901656]

35. Radley JJ, Anderson RM, Hamilton BA, Alcock JA, Romig-Martin SA (2013): Chronic Stress-Induced Alterations of Dendritic Spine Subtypes Predict Functional Decrements in an Hypothalamo–Pituitary–Adrenal-Inhibitory Prefrontal Circuit. J Neurosci 33: 14379–14391. [PubMed: 24005291]

36. McEwen BS, Morrison JH (2013): Brain On Stress: Vulnerability and Plasticity of the Prefrontal Cortex Over the Life Course. Neuron 79: 16–29. [PubMed: 23849196]

37. LeGates TA, Kvarta MD, Tooley JR, Francis TC, Lobo MK, Creed MC, Thompson SM (2018): Reward behaviour is regulated by the strength of hippocampus–nucleus accumbens synapses. Nature 564: 258–262. [PubMed: 30478293]

38. Covington HE, Lobo MK, Maze I, Vialou V, Hyman JM, Zaman S, et al. (2010): Antidepressant effect of optogenetic stimulation of the medial prefrontal cortex. J Neurosci 30: 16082–90. [PubMed: 21123555]

39. McNamara B, Ray JL, Arthurs OJ, Boniface S (2001): Transcranial magnetic stimulation for depression and other psychiatric disorders. Psychol Med 31.

40. Bosch M, Castro J, Saneyoshi T, Matsuno H, Sur M, Hayashi Y (2014): Structural and molecular remodeling of dendritic spine substructures during long-term potentiation. Neuron 82: 444–459. [PubMed: 24742465]

41. Bello-Medina PC, Flores G, Quirarte GL, McGaugh JL, Prado Alcalá RA (2016): Mushroom spine dynamics in medium spiny neurons of dorsal striatum associated with memory of moderate and intense training. Proc Natl Acad Sci U S A 113: E6516–E6525. [PubMed: 27698138]

42. Bourne J, Harris KM (2007): Do thin spines learn to be mushroom spines that remember? Curr Opin Neurobiol 17: 381–386. [PubMed: 17498943]

43. Tashiro A, Minden A, Yuste R (2000): Regulation of dendritic spine morphology by the rho family of small GTPases: antagonistic roles of Rac and Rho. Cereb cortex 10: 927–938. [PubMed: 11007543]

44. Khibnik LA, Beaumont M, Doyle M, Heshmati M, Slesinger PA, Nestler EJ, Russo SJ (2016): Stress and Cocaine Trigger Divergent and Cell Type-Specific Regulation of Synaptic Transmission at Single Spines in Nucleus Accumbens. Biol Psychiatry 79: 898–905. [PubMed: 26164802]

45. Grueter BA, Robison AJ, Neve RL, Nestler EJ, Malenka RC (2013): FosB differentially modulates nucleus accumbens direct and indirect pathway function. Proc Natl Acad Sci U S A 110: 1923–1928. [PubMed: 23319622]

46. Vialou V, Robison AJ, Laplant QC, Covington HE 3rd, Dietz DM, Ohnishi YN, et al. (2010): DeltaFosB in brain reward circuits mediates resilience to stress and antidepressant responses. Nat Neurosci 13: 745–752. [PubMed: 20473292]

47. Lobo MK, Zaman S, Damez-Werno DM, Koo JW, Bagot RC, DiNieri JA, et al. (2013): DeltaFosB induction in striatal medium spiny neuron subtypes in response to chronic pharmacological, emotional, and optogenetic stimuli. J Neurosci 33: 18381–18395. [PubMed: 24259563]

48. Christoffel DJ, Golden SA, Dumitriu D, Robison AJ, Janssen WG, Ahn HF, et al. (2011): I B Kinase Regulates Social Defeat Stress-Induced Synaptic and Behavioral Plasticity. J Neurosci 31: 314–321. [PubMed: 21209217]

49. Turrigiano GG (2008): The self-tuning neuron: synaptic scaling of excitatory synapses. Cell 135: 422–435. [PubMed: 18984155]

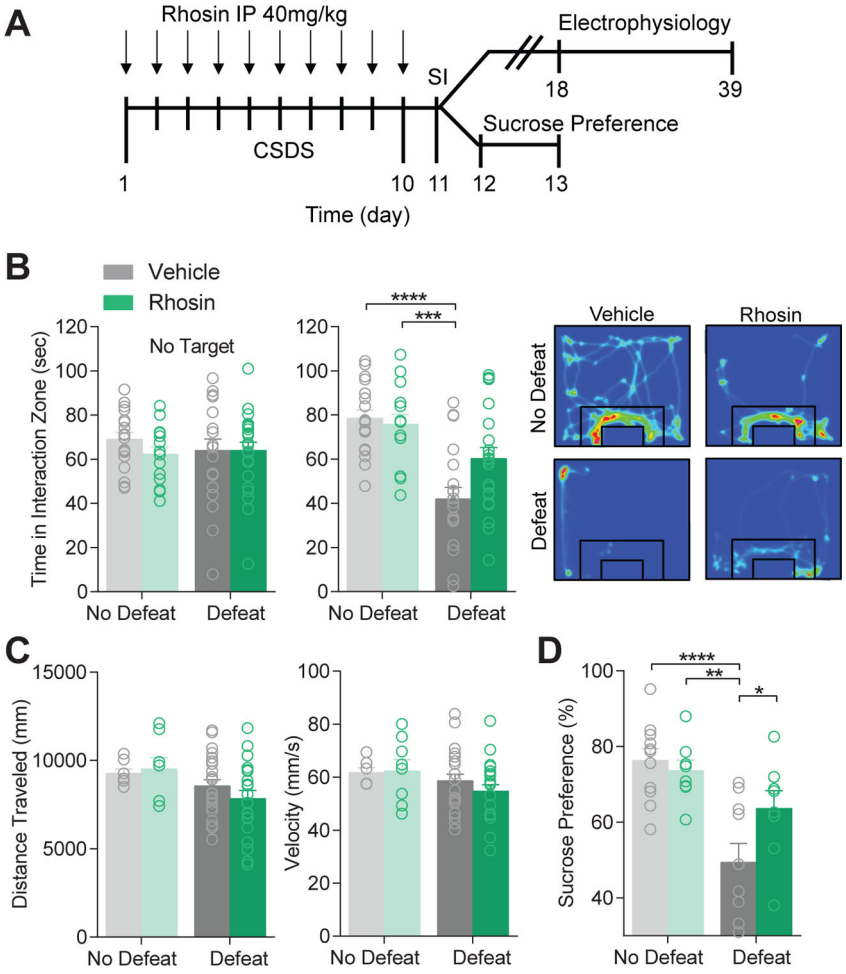

Figure 1. Rhosin blocks stress-induced susceptibility.

(A) Timeline for CSDS, social interaction (SI), and subsequent electrophysiology or sucrose preference. **(B)** Rhosin treatment prevents social avoidance caused by social defeat stress (No Target: $P>0.05$; Target: $P<0.05$; N=16–23 mice per group). Representative heat plots display movement of mice around a social target where warm colors represent more time and cool colors represent less time. **(C)** No difference was observed in distance traveled ($P>0.05$) or velocity ($P>0.05$; N=16–23 mice per group). **(D)** Rhosin prevented reduced sucrose preference caused by CSDS ($P<0.05$; N=8–11 mice per group). For exact statistics see Supplemental Table 1.

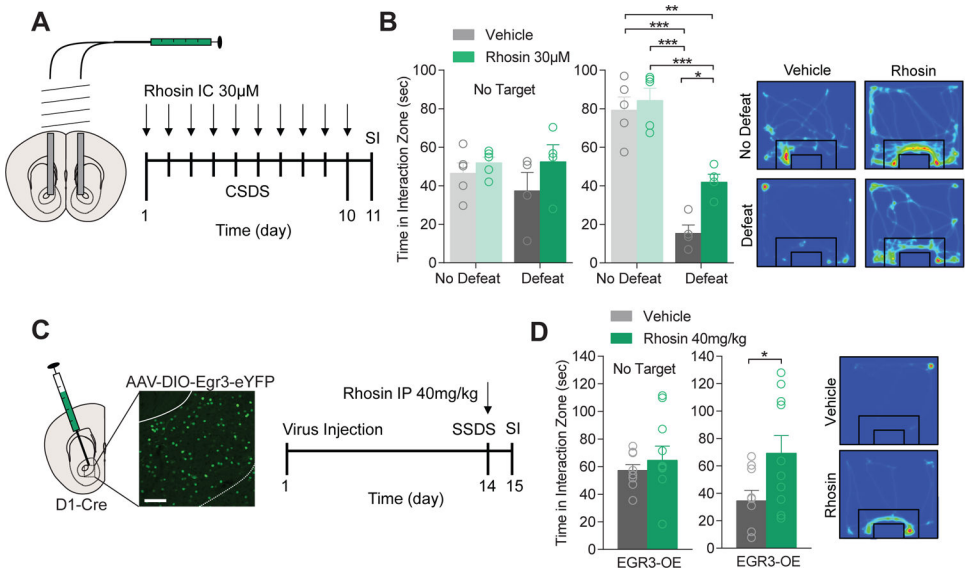

Figure 2. NAc Rhosin infusion blocks stress-induced susceptibility and is dependent on D1-MSN EGR3 expression.

(A) Schematic of NAc Rhosin infusion and timeline for treatment. **(B)** Infusion of Rhosin in the NAc attenuates stress-induced social avoidance (No Target: $P>0.05$; Target: $P<0.05$; N=4–5 mice per group). **(C)** Injection site of EGR3 overexpression (EGR3-OE) virus within the NAc of D1-Cre mice and timeline for treatment (scale bar 100μm). **(D)** SSDS reduced social interaction in mice overexpressing EGR3 in NAc D1-MSNs which was blocked by Rhosin treatment ($P<0.05$; N=9,10 mice per group). For exact statistics see Supplemental Table 1.

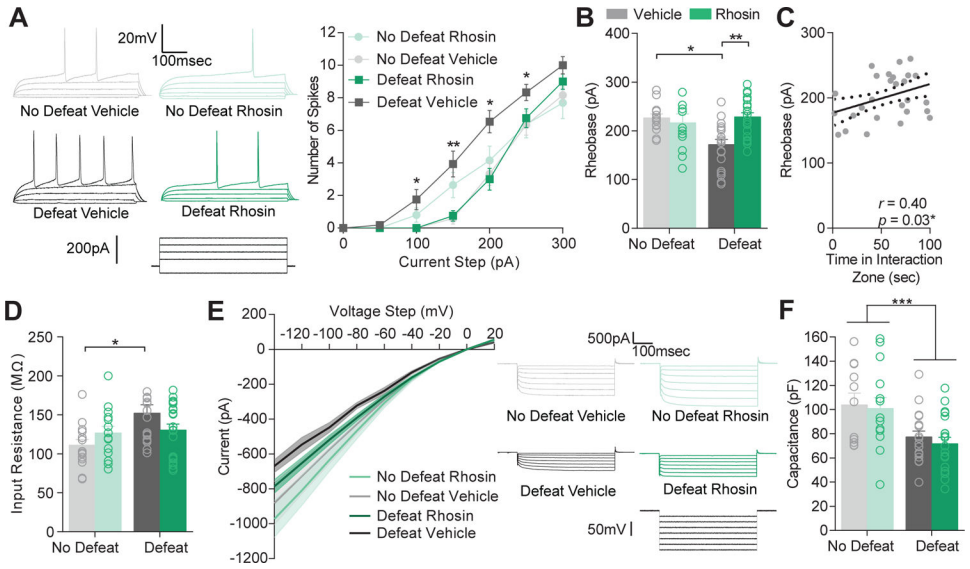

Figure 3. Rhosin blocks stress-induced hyperexcitability in NAc D1-MSNs.

(A) Current (−50 to 300 pA) was injected in to NAc D1-MSNs from non-defeat or defeat mice treated with vehicle or Rhosin. Representative traces with current injection (50–200 pA) from each condition are shown. Rhosin blocked hyperexcitability observed in defeat mice treated with vehicle ($P<0.0001$). **(B)** Reduced rheobase is prevented by Rhosin treatment ($P<0.01$; **(C)** Rheobase positively correlates with time spent in the interaction zone ($P<0.05$). **(D)** Enhanced input resistance is blocked by Rhosin ($P<0.05$). **(E)** Evoked plateau currents (the point at which current stabilizes in response to a negative voltage pulse) from voltage clamp steps (−140 to 20mV) were smaller in defeat vehicle mice but not mice treated with Rhosin ($P<0.0001$). **(F)** Capacitance was significantly reduced in all defeat animals (Interaction $P>0.05$; Main effect of defeat $P<0.001$; for all experiments N/n= 4–7/12–20). For exact statistics see Supplemental Table 1.

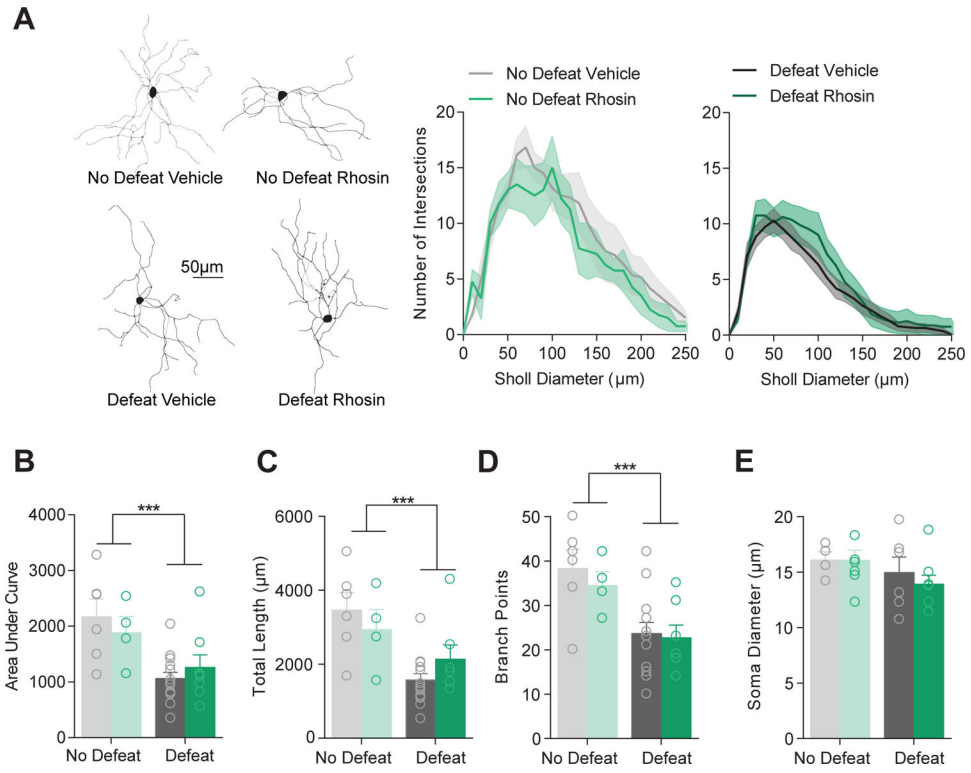

Figure 4. Rhosin has no effect on dendritic atrophy caused by stress.

(A) Sholl profiles show no treatment difference in concentric ring intersections (10 μm) with dendritic branches. **(B)** No difference in the area under the curve of sholl plots was observed when comparing across treatment conditions (Interaction $P>0.05$; Main effect of defeat $P<0.001$). **(C)** Total dendritic length is not different across treatment (Interaction $P>0.05$; Main effect of defeat $P<0.001$). **(D)** Dendritic branch points are not different across treatment (Interaction $P>0.05$; Main effect of defeat $P<0.001$; N= 4–14 cells per group). **(E)** The soma diameter of cells is not different across defeat or treatment ($P>0.05$; N=4–9 cells per group). For exact statistics see Supplemental Table 1.

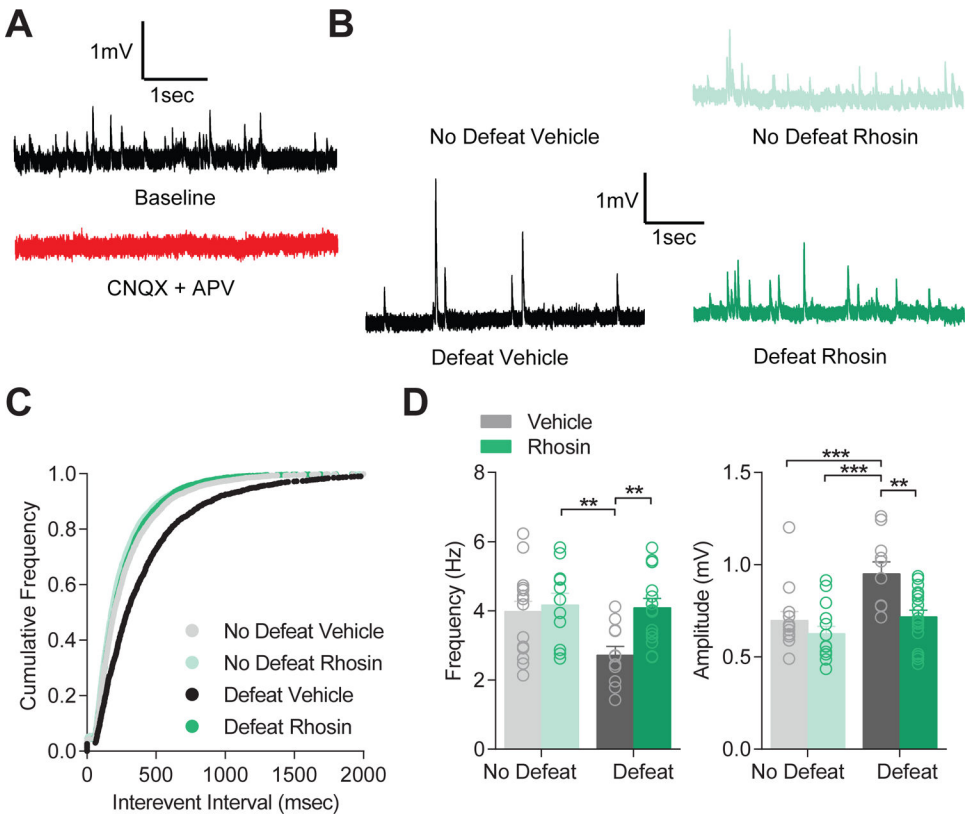

Figure 5. Rhosin prevents decreased excitatory transmission on NAc D1-MSNs.

(A) CNQX and APV blocked all spontaneous events indicating spontaneous events are excitatory. **(B)** Representative traces of sEPSPs. **(C)** Cumulative frequency plot demonstrating Rhosin restored normal sEPSP frequency while vehicle treated animals displayed elevated frequency (K-S test defeat Rhosin vs defeat vehicle: $P<0.0001$). **(D)** Rhosin blocked reduced frequency of sEPSPs ($P<0.05$) and enhanced amplitude of sEPSPs ($P<0.05$; N/n= 3–6/11–18 cells per group) caused by stress. For exact statistics see Supplemental Table 1.

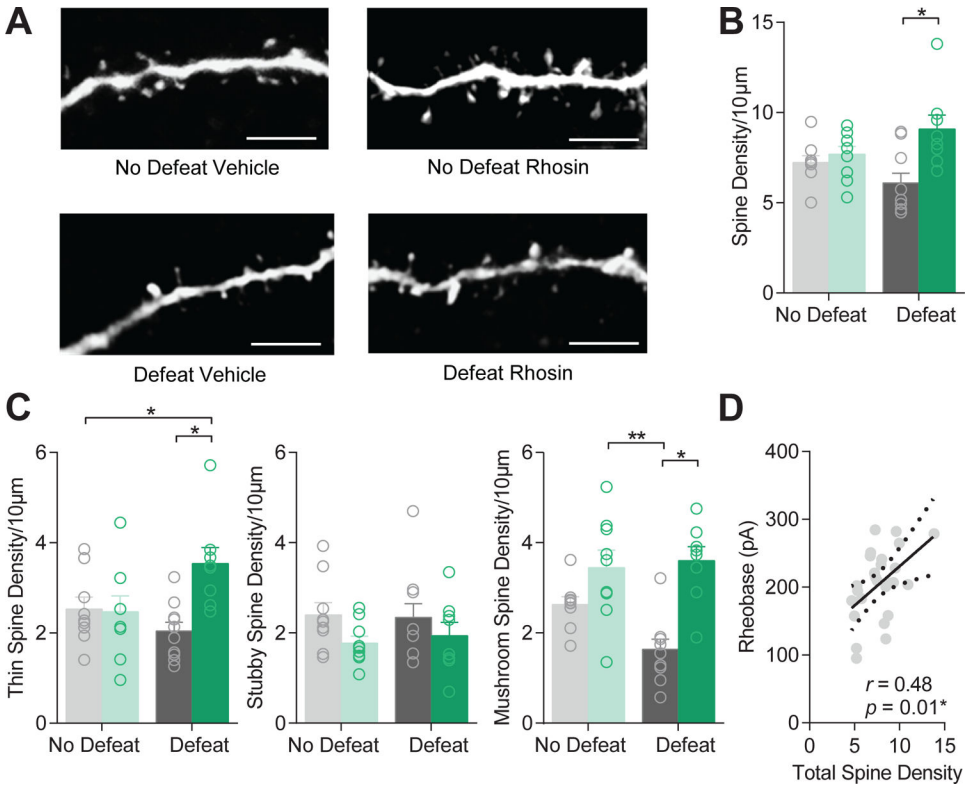

Figure 6. Rhosin enhances spine density in defeat mice.

(A) Representative images of spines (scale bar 5µm). **(B)** Spine density is significantly enhanced by Rhosin treatment in defeat mice ($P<0.05$). **(C)** Thin spine density ($P<0.05$) and mushroom spine density ($P<0.05$), but not stubby spine density ($P>0.05$) is enhanced by Rhosin treatment (N=8–10 cells per group). **(D)** Rheobase significantly correlates with total spine density ($P<0.05$). For exact statistics see Supplemental Table 1.